

## AN ANALYTICAL SOLUTION FOR SOLID STRESSES IN A SILO WITH AN INNER TUBE

J.F. CHEN<sup>1</sup>, J.Y. OOI<sup>2</sup>, J.M. ROTTER<sup>2</sup>, M. BATIKHA<sup>3</sup> AND G. HORRIGMOE<sup>4</sup>

<sup>1</sup> School of Planning, Architecture and Civil Engineering, Queen's University Belfast, Belfast, BT9 5AG, Northern Ireland, UK  
E-mail: [j.chen@qub.ac.uk](mailto:j.chen@qub.ac.uk)

<sup>2</sup> Institute for Infrastructure and Environment, School of Engineering, The University of Edinburgh, EH9 3JL, Scotland, U.K

<sup>3</sup> Structural Engineering Department, Faculty of Civil Engineering, Damascus University, Syria

<sup>4</sup> Sweco Norge, Narvik NO-8514, Norway

**Key words:** Bulk solid, silo, silo with internal tube, anti-dynamic tube, stresses, silo pressure.

**Abstract.** This paper presents an analytical solution for the solid stresses in a silo with an internal tube. The research was conducted to support the design of a group of full scale silos with large inner concrete tubes. The silos were blasted and formed out of solid rock underground for storing iron ore pellets. Each of these silos is 40m in diameter and has a 10m diameter concrete tube with five levels of openings constructed at the centre of each rock silo. A large scale model was constructed to investigate the stress regime for the stored pellets and to evaluate the solids flow pattern and the loading on the concrete tube. This paper focuses on the development of an analytical solution for stresses in the iron ore pellets in the silo and the effect of the central tube on the stress regimes. The solution is verified using finite element analysis before being applied to analyse stresses in the solid in the full scale silo and the effect of the size of the tube.

### 1 INTRODUCTION

Internal tubes are some times placed inside silos for various purposes such as reducing or eliminating vibration on a silo structure arisen from discharge. When the internal tube is small relatively to the silo diameter, its presence will have little effect on the stress distribution outside the tube. Since the magnitude of solid stresses inside a long tube is proportional to tube diameter, the solid stresses inside a small inner tube is very small during both filling and discharge. The effect of the presence of the inner tube on stresses in a silo is therefore typically not a significant issue, especially for relatively small silos. This may explain why research on pressures in silos with central tube is rare, despite a large volume of literature on the topic [1-4].

A new use of inner tube was proposed when we conducted research for LKAB in support of their design of a group of very large silos. The silos were required to have very large storage capacity to meet LKAB's operational needs, but it was realised that very high stresses would be experienced in the stored solids in these large silos. This led to major concerns with

the effect on product quality, as the stored product could undergo significant degradation during discharge under high shear stresses. It was proposed that a large tube structure with windows was constructed inside the large silo, so that all solids are filled and discharged through the inner tube, leaving the solids between the inner tube and the outer silo wall stationary during discharge except those near the top surface which are under minimal pressure.

Because the silos considered had different sizes, a natural question was when an inner tube is needed and when it is not, to ensure that the stresses within the solid is limited to certain values. Other questions included what size the internal tube needed to be and how its size would affect the stresses in the solid. This paper presents an analytical solution developed to answer these questions. The solution is compared with a finite element analysis for verification and then applied to a full scale silo to investigate the effect of the size of the internal tube.

## 2 EQUILIBRIUM BASED ON THE METHOD OF DIFFERENTIAL SLICES

### 2.1 Geometry and material properties

Figure 1 shows a silo with height  $H_o$  and radius  $R_o$ . It has an internal tube with height  $H_i$  and radius  $R_i$ . The silo is filled with a cohesionless solid which has a density  $\gamma$  and an effective internal frictional angle  $\phi$ . The frictional coefficient between the solid and the external wall is  $\mu_o = \tan\phi_w$ . The friction is assumed to be fully mobilised against both the outer silo walls and the inner tube walls.

It is further assumed that both the normal wall pressure and the frictional stresses around the circumferences of both the inner wall of the outer silo, and the outer wall of the inner tube, are uniform. Note that although a central tube in a cylindrical silo is analysed here, the same solution is applicable to other geometrical configurations such as a circular tube in a square silo, subject to that the above assumptions are valid.

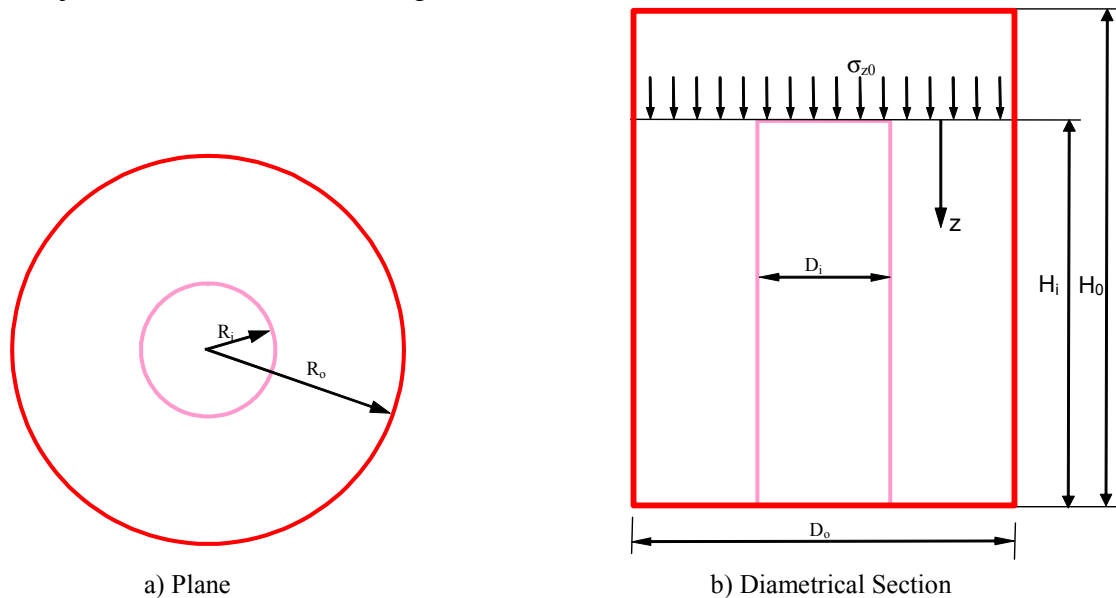


Figure 1 Geometry of the silo

## 2.2 Governing equation

Similar to pressure analyses of cylindrical silos and conical hoppers [5-7], a differential equation can be established based on the vertical equilibrium of an infinitesimal horizontal slice at a given depth  $z$  (Figure 2). Here the vertical axis  $z$  is taken to originate from the top end of the internal tube and is positive downwards. Assuming that the normal pressure on the wall of the outer silo is  $p_{zno}$  and that on the outer wall of the inner tube is  $p_{zni}$ , and that the wall friction is fully mobilised everywhere, the following governing equation can be established based on vertical equilibrium of the infinitesimal horizontal slice (Figure 2):

$$\frac{d\sigma_z}{dz} + \frac{1}{z_o} \sigma_z = \gamma \quad (1)$$

where the characteristic depth

$$z_o = \frac{A}{\mu_o k_o M_o + \mu_i k_i M_i} \quad (2)$$

in which  $M_o$  and  $M_i$  are respectively the perimeter of the outer silo wall and the inner tube wall,  $A$  is the cross sectional area of the slice,  $\mu_o$  and  $\mu_i$  are respectively the frictional coefficient between the outer silo wall and the solids and between the outer wall of the internal tube and the solids,  $k_o$  and  $k_i$  are respectively the lateral pressure ratio (the ratio of the horizontal wall pressure to the average vertical stress across the horizontal plane at the given depth  $z$ ) at the wall of the outer silo and the wall of the inner tube.

For a cylindrical silo with a cylindrical inner tube, Equation 2 can be expressed as

$$z_o = \frac{\pi(R_o^2 - R_i^2)}{\mu_o k_o 2\pi R_o + \mu_i k_i 2\pi R_i} = \frac{R_o^2 - R_i^2}{2\mu_o k_o R_o + 2\mu_i k_i R_i} \quad (3)$$

If there is no internal tube,  $R_i=0$ , Equation 3 reduces to  $z_o = \frac{R_o}{2\mu_o k_o}$  which is the same as that in the Janssen's [5] solution.

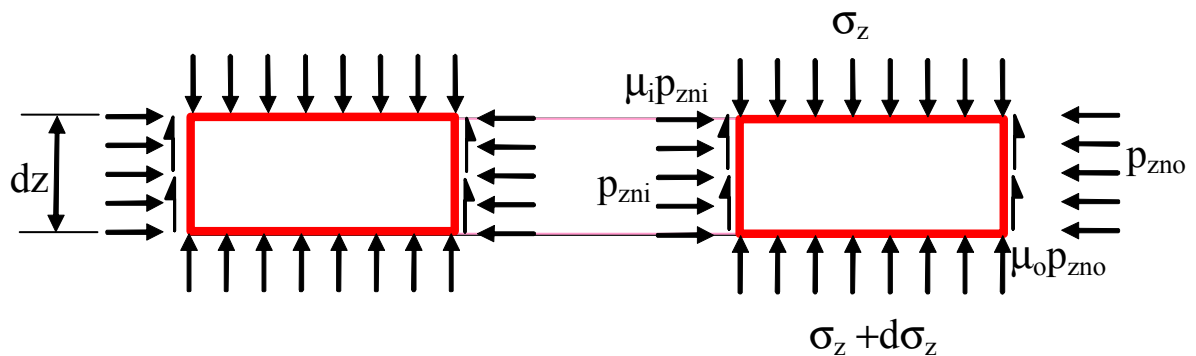


Figure 2: Stresses on a horizontal slice

### 3 SOLUTION

The general solution of Equation 2 is

$$\sigma_z = \gamma z_o + C e^{-\frac{z}{z_o}} \quad (4)$$

If a uniform vertical stress  $\sigma_{z0}$  is acting on the solid at  $z=0$ , the boundary condition can be expressed as

$$z=0, \sigma_z = \sigma_{z0} \quad (5)$$

The constant C in Equation 4 can be found by substituting it into Equation 5:

$$C = \sigma_{z0} - \gamma z_o \quad (6)$$

Substituting Equation 6 into Equation 4 gives

$$\sigma_z = \gamma z_o \left[ 1 + \left( \frac{\sigma_{z0}}{\gamma z_o} - 1 \right) e^{-\frac{z}{z_o}} \right] \quad (7)$$

Once the vertical stress in the solid is obtained from Equation 7, the normal pressure on the inner wall of the outer silo can be obtained from  $p_{zno} = k_o \sigma_z$  and that on the outer wall of the inner silo  $p_{zni} = k_i \sigma_z$ .

### 4 FINITE ELEMENT ANALYSES

A finite element stress analysis of a large scale model steel silo with a central acrylic tube was conducted to verify and compare with the above analytical solution. Details of the model silo are shown in Figure 3. Mini iron ore pellets with a mean size of 3.0 mm specially manufactured by LKAB Laboratories for this study were used in the experiments. The mini pellets were tested to have a density  $\gamma = 23 \text{ kN/m}^3$ , angle of repose  $\phi_r = 29^\circ$  and effective internal frictional angle  $\phi = 26^\circ$ . The friction coefficient between the mini pellets and both the outer silo wall and inner tube wall was measured to be  $\mu = 0.488$  (i.e. wall friction angle =  $26^\circ$ ). Only the filling condition was modelled in the FE analyses. Both the inner tube and the outer silo were filled with the mini pellets to form a top surface profile as shown in Figure 3b.

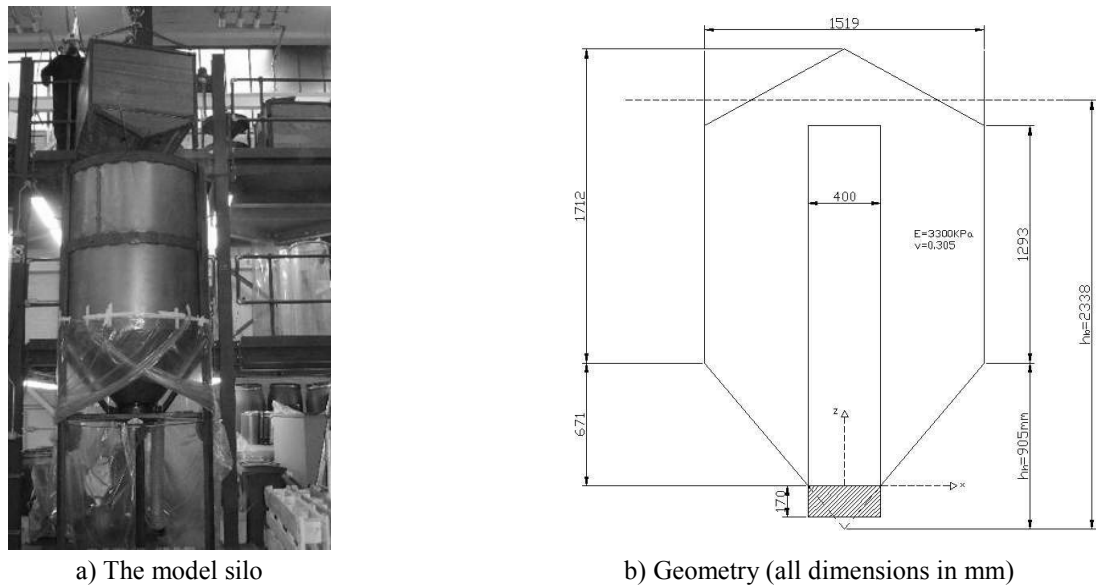


**Figure 3: A 1:25 scale model silo**

ABAQUS Version 6.5-4 [8] was used to conduct the FE analyses. The silo, tube, iron ore pellets and the supporting structure (which consisted of steel sockets, epoxy and steel trusses) were all modelled as linear elastic materials, but the problem was nonlinear due to nonlinear frictional interaction between the pellets and the silo and tube walls. The 8-node quadratic axisymmetric solid element CAX8 was used to model the silo, tube and the pellets. The contact surfaces between the pellets and both the silo and tube walls were modelled using the 3-node axisymmetric slide line element ISL22A, which is compatible with element CAX8. The axisymmetric axis was restrained against horizontal displacement assuming axisymmetry of the problem. The vertical displacement was restrained at the hopper/cylinder transition which was supported by columns. Previous research has shown that different loading processes have insignificant effect on the predicted storing stress distributions in the solid [9,10]. The self weight of the pellets was thus applied incrementally as switch-on gravity (i.e. all the solid was assumed to be in place before the gravity is switched on). Further details of the FE analyses can be found in [11].

## 5 COMPARISON BETWEEN ANALYTICAL AND FEA PREDICTIONS

A comparison between the FEA predictions and the analytical solution for the model silo with a central tube is presented in this section.

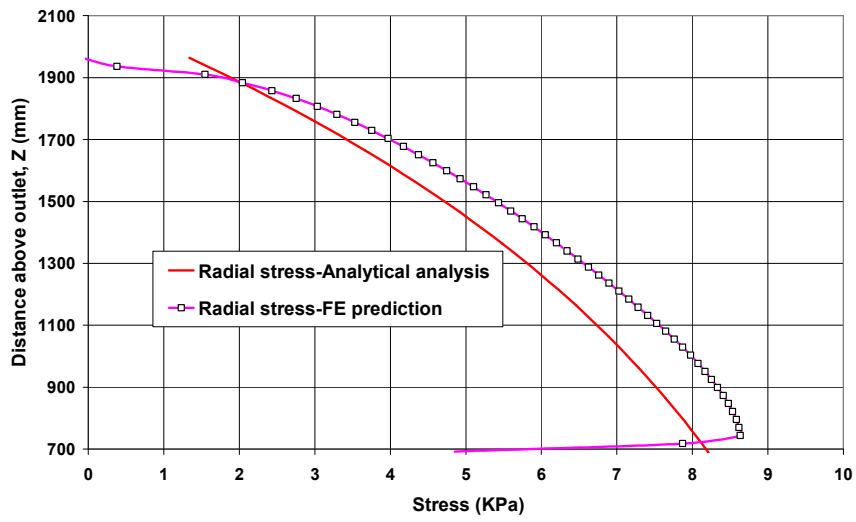


Figure 4: Solid radial stress near the silo wall ( $k_o=0.44$ ,  $k_i=0.65$ )

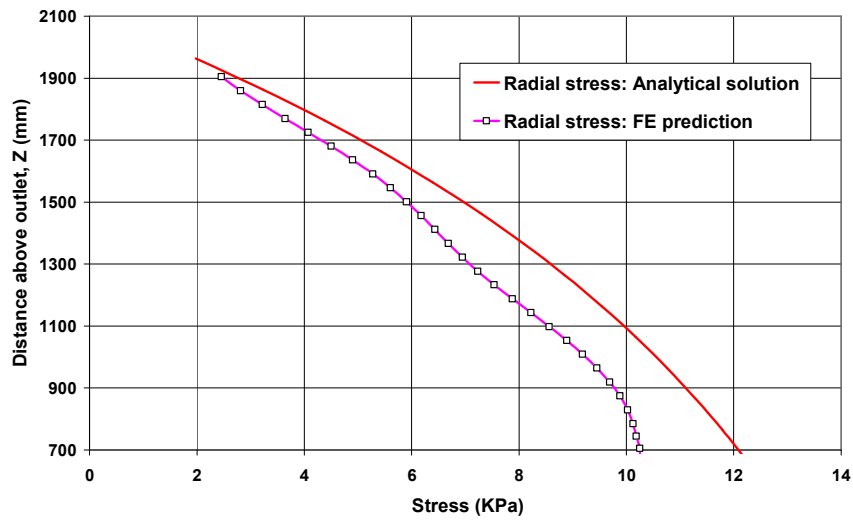


Figure 5: Solid radial stress near the tube ( $k_o=0.44$ ,  $k_i=0.65$ )

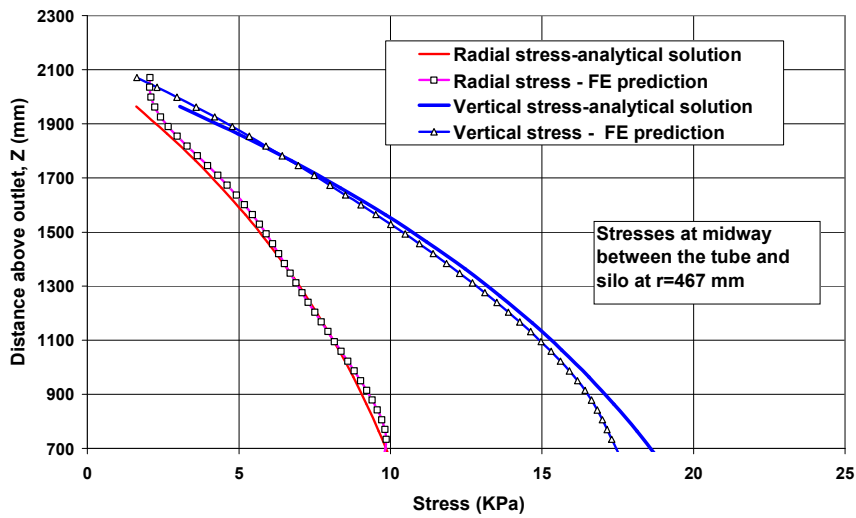


Figure 6: Solid stress at mid-way between the silo and the tube ( $k_o=0.44$ ,  $k_i=0.65$ )

The FEA predictions show that  $k_o=0.44$  and  $k_i=0.65$  which gives a weighted mean value of  $k$  close to 0.53 which was used to calculate the Poisson's ratio in the FE calculation [11]. Some comparisons are shown in Figures 4-6. Figure 4 shows the radial stress in the pellets near the silo wall. It shows that for the given parameters, the analytical prediction is slightly lower than the FE predictions. In contrast, the analytical prediction is slightly higher than the FE predictions near the tube (Figure 5). In the mid-way between them, the analytical solution is in a very close agreement with the FE predictions. This is understandable because the analytical solution is based on the global equilibrium. Note that the radial stress in Figure 6 was obtained by multiplying the mean vertical stress from the analytical solution (shown in the same figure) by the lateral pressure ratio of 0.53 which was obtained from material testing and used in the FEA to obtain the Poisson's ratio.

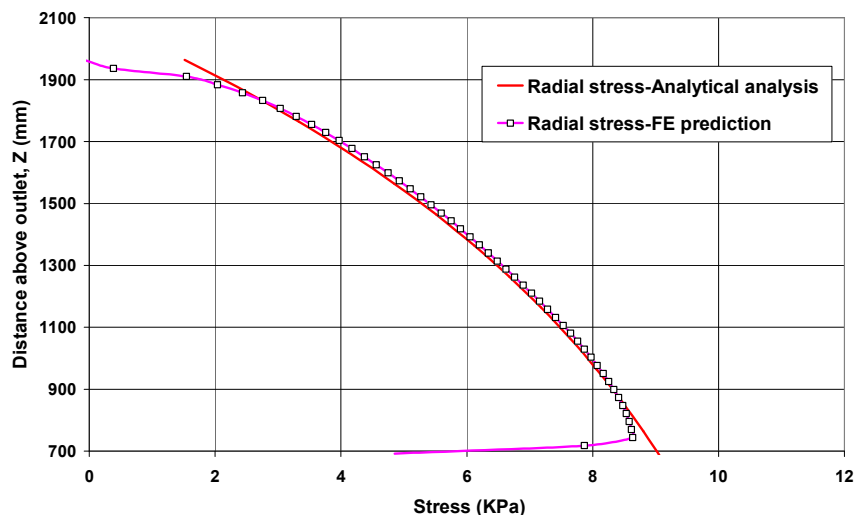


Figure 7: Solid stress near the silo wall ( $k_o=0.5$ ,  $k_i=0.57$ )

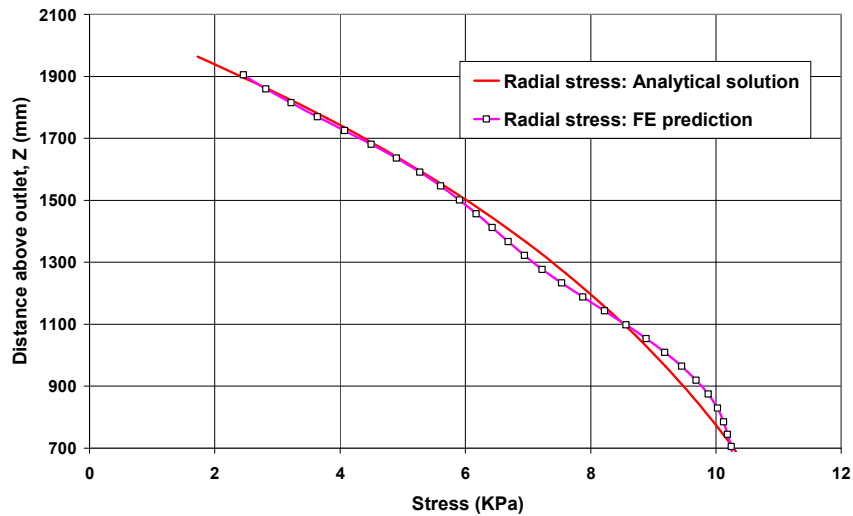


Figure 8: Solid stress near the tube ( $k_o=0.5$ ,  $k_i=0.57$ )

The radial stress is in very close agreement everywhere between the FE predictions and the analytical solution by adopting  $k_o=0.5$ ,  $k_i=0.57$ , as shown in Figures 7 and 8.

For simplicity, one may adopt  $k_o=k_i=0.53$ . This has an additional advantage that  $k=0.53$  is a value obtained from material tests. The analytical solution very slightly over predicts the silo wall pressures (Figure 9) but slightly under predict the outer wall pressures of the tube (Figure 9). Such small differences can well be catered for in design situations.

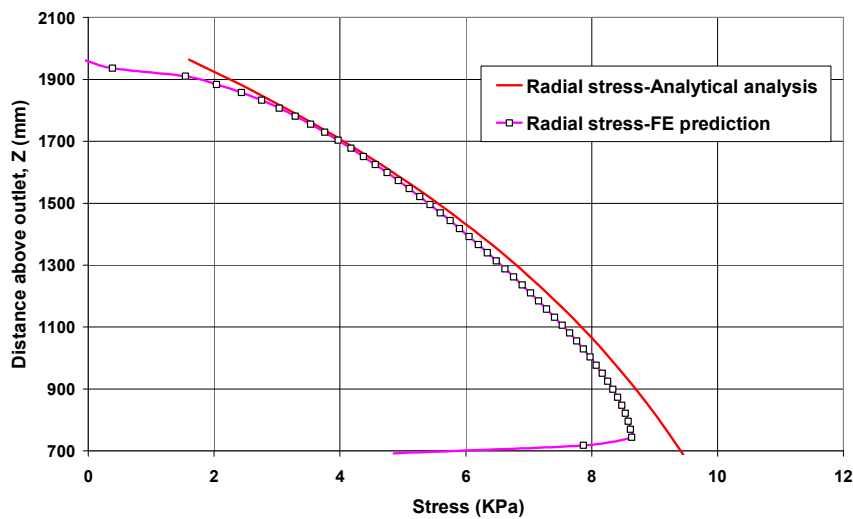


Figure 8: Solid stress near the silo wall ( $k_o=k_i=0.53$ )



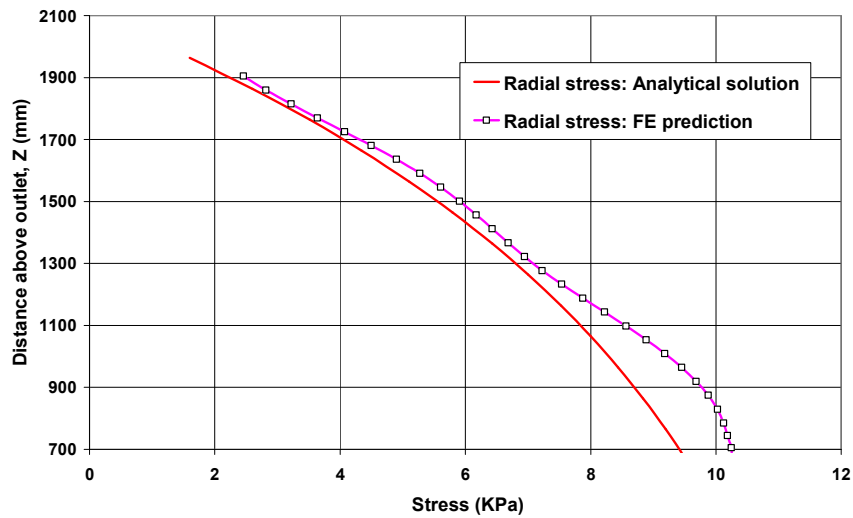


Figure 9: Solid stress near the tube ( $k_o=k_i=0.53$ )

Figure 10 shows the normal pressure and frictional traction along the whole height of the silo wall. The analytical predictions of these values in the hopper section are based on the Eurocode design equations [12] and Rotter [13] under filling condition for normal hoppers without a central tube. In the hopper section, the analytical solution is in very close agreement with the FE predictions near the hopper/cylinder transition. It over-predicts the wall pressures further down the hopper, but this has minimal implications for solid handling design because the stresses there are much smaller than those near the transition.

In practical design, appropriate upper and lower characteristic values of each parameter should be considered. For example, when designing the tube wall, upper characteristic value for  $k_i$  and lower characteristic value for  $k_o$  may be adopted to give higher design pressures. Other parameters such as the wall friction coefficients should be similarly considered.

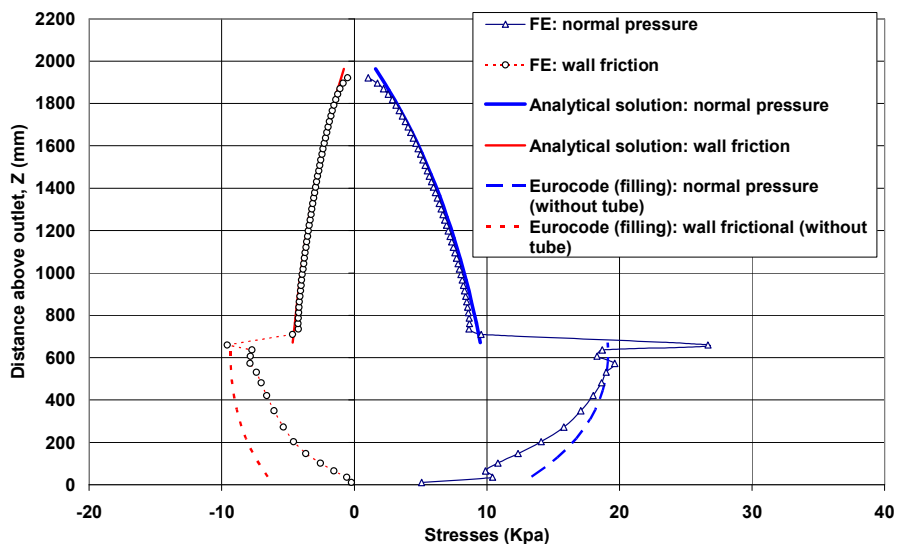


Figure 10: Wall pressure and friction: FE versus analytical predictions ( $k_o=k_i=0.53$ )

## 6 STRESSES IN A FULL SCALE SILO

The analytical solution developed above was used to predict the pellet stresses in the full scale silo (i.e. the full scale of the silo shown in Figure 3), but with varying size of the tube. The  $k$  value was taken to be 0.5 at the silo wall and 0.57 at the tube which were found to match best with the finite element predictions were used in the calculations, together with a wall friction angle of  $30^\circ$ . It is seen that the size of the tube has a significant effect on the wall pressures (Figure 11) and the mean vertical stress in the silo (Figure 12) when the tube is large.

Note that in Figures 11 and 12 a uniform vertical stress was applied at the level at the top of the tube, reflecting the stress induced by the solid above the top of the tube. The height of the internal tube naturally affects this stress. In design, the height of the internal tube may be optimised to reduce the constructional cost of the tube, whilst give satisfactorily stress levels in the solid.

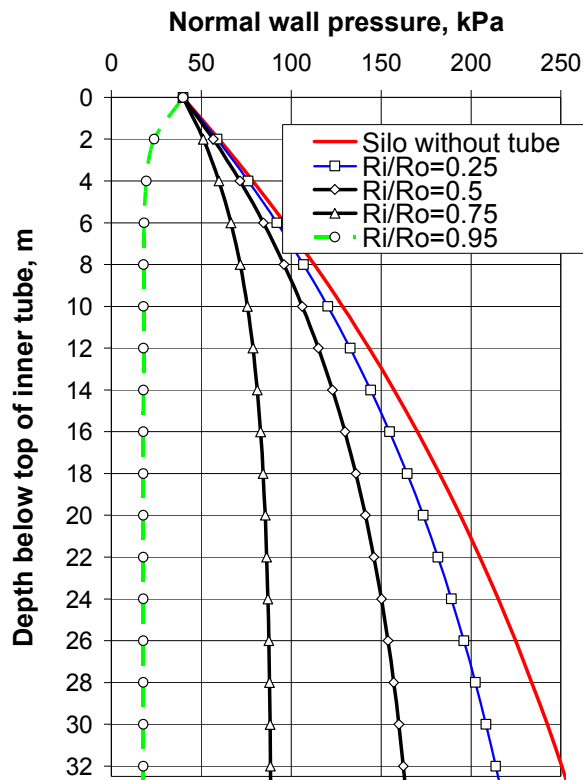


Figure 11: Effect of tube size on wall pressures in a full scale silo

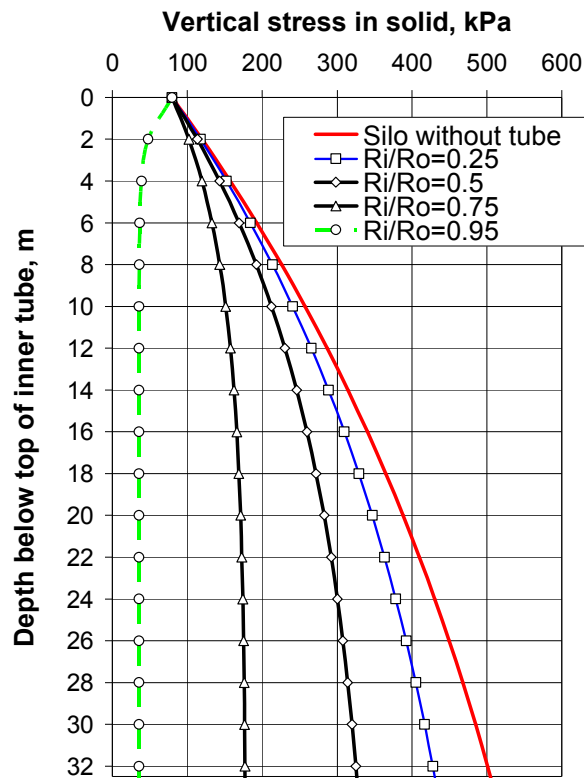


Figure 12: Effect of tube size on solid vertical stress in a full scale

## 7 CONCLUSIONS

An approximate analytical solution for solid stresses in a silo with an inner tube has been developed based on the method of differential slices. Finite element analyses have also been conducted for a large model silo. The analytical predictions are in close agreement with those obtained from the FE analyses. The analytical solution is thus verified.

The presence of the tube may or may not significantly reduce the wall pressures and vertical stresses in the solid in the cylindrical section, depending on the geometrical design and a range of material parameters such as lateral pressure ratios, wall friction coefficients etc. This analytical solution is a powerful tool which can be used to develop and optimise the design by adjusting the design parameters.

Furthermore, the presence of the tube can significantly reduce the stresses in the solid in the hopper section. Adopting the Eurocode hopper design method for a hopper without a tube would be conservative. In addition, loading from the tube to the hopper wall must also be considered.

## 8 ACKNOWLEDGEMENTS

The work presented in this paper was contracted by LKAB, Malmberget, Sweden. Financial support and permission for publishing the results from LKAB are gratefully acknowledged.

## REFERENCES

- [1] Schulze, D. and Schwedes, J. Tests on the Application of Discharge Tubes. *Bulk solids handling* (1992), 12(1).
- [2] Jöhnk, V.H. Reduzierung von Erschütterungen beim Abzug aus Klinkersilos (reduction of vibrations associated with clinker silo discharge). *ZEMENT-KALK-GIPS* (1985), 38 (11):657-659.
- [3] Schulze, D. and Schwedes, J. Tests on the application of discharge tubes. *Bulk Solids Handling* (1992), 12(1):33.
- [4] Schulze, D., Leonhardt, C., Kossert, J. and Schwedes, J. Design of a Silo for the Storage of 10,000 t Sulphur Granules. *Bulk Solids Handling* (1998), 18(2):211.
- [5] Janssen, H.A. Versuche über Getreidedruck in Silozellen. *Zeitschrift des Vereines Deutscher Ingenieure* (1895) 39(35):1045-1049.
- [6] Walker, D.M. An approximate theory for pressure and arching in hoppers. *Chemical Engineering Science* (1966), 21:975-997.
- [7] Walters, J.K. A theoretical analysis of stresses in axially-symmetric hoppers and bunkers. *Chemical Engineering Science* (1973), 28(3):779-789.
- [8] *ABAQUS User's Manual*, Version 6.5-4. Hibbit, Karlsson and Sorensen Co., USA, (2006).
- [9] Chen, J.F., S.K. Yu, Ooi, J.Y. and Rotter, J.M. Finite element modelling of filling pressures in a full-scale silo. *Journal of Engineering Mechanics, ASCE* (2001), 127(10):1058-1066.
- [10] Yu, S.K. *Finite element prediction of wall pressures in silos*. PhD thesis, Wolverhampton University, (2003).
- [11] Chen, J.F., Ooi, J.Y., Rotter, J.M., Batikha, M., Zhong, Z., Andreasson, B., Forsmo, S.E., Tano, K. and Horrigmoe, G. Finite element analysis of solid stresses in a silo with an inner tube. *Proc. of the 6th International Conference for Conveying and Handling of Particulate Solids (CHoPS) and the 10th International Conference on Bulk Materials Storage, Handling & Transportation (ICBMH)*, 3–7 Aug. 2009, Brisbane, Australia, 713-718.
- [12] EN 1991-4. *Eurocode 1: Basis of Design and Actions on Structures, Part 4 - Silos and Tanks, Eurocode 1 Part 4*. CEN. Brussels (2005).
- [13] Rotter, J.M. *Guide for the economic design of circular metal silos*, Spon Press, London (2001).